



Technological University Dublin
ARROW@TU Dublin

Articles

School of Food Science and Environmental
 Health

2015

Mechanism of Inactivation by High Voltage Atmospheric Cold Plasma Differs between Escherichia coli and Staphylococcus aureus

Lu Han

Technological University Dublin, lu.han@tudublin.ie

Sonal Patil

Technological University Dublin, sonalpatil81@gmail.com

Daniela Boehm

Technological University Dublin, daniela.boehm@tudublin.ie

vladimir Milosavljević

Technological University Dublin, vm@tudublin.ie

Follow this and additional works at: <https://arrow.tudublin.ie/schfsehart>

Patrick Cullen

Technological University of Dublin, picullen@tudublin.ie



Part of the [Biotechnology Commons](#), and the [Other Microbiology Commons](#)

See next page for additional authors

Recommended Citation

Han, L. et al. (2015) Mechanism of Inactivation by High Voltage Atmospheric Cold Plasma Differs between Escherichia coli and Staphylococcus aureus. *Applied and environmental microbiology*, Published online 2015. DOI:10.1128/AEM.02660-15

This Article is brought to you for free and open access by the School of Food Science and Environmental Health at ARROW@TU Dublin. It has been accepted for inclusion in Articles by an authorized administrator of ARROW@TU Dublin. For more information, please contact yvonne.desmond@tudublin.ie, arrow.admin@tudublin.ie, brian.widdis@tudublin.ie.



This work is licensed under a [Creative Commons Attribution-Noncommercial-Share Alike 3.0 License](#)



Authors

Lu Han, Sonal Patil, Daniela Boehm, vladimir Milosavljević, Patrick Cullen, and Paula Bourke

1 **Mechanism of Inactivation by High Voltage Atmospheric Cold Plasma Differs**
2 **between *Escherichia coli* and *Staphylococcus aureus***

3

4 **Running title: Inactivation Mechanism of Atmospheric Cold Plasma**

5

6 Han, L.¹, Patil, S.¹, Boehm, D.¹, Milosavljević, V.¹, Cullen, P.J.^{1,2}, & Bourke, P.^{1#}

7

8 1. *School of Food Science and Environmental Health, Dublin Institute of*

9 *Technology, Ireland*

10 2. *School of Chemical Engineering, UNSW, Sydney, Australia*

11 **Correspondence:**

12 # Paula Bourke, Dublin Institute of Technology, Cathal Brugha Street, Dublin 1,
13 Ireland.

14 Tel: +353 1 4027594

15 E-mail: paula.bourke@dit.ie

Abstract:

Atmospheric cold plasma (ACP) is a promising non-thermal technology effective against a wide range of pathogenic microorganisms. Reactive oxygen species (ROS) play a crucial inactivation role when air or other oxygen containing gases are used. With strong oxidative stress, cells can be damaged by lipid peroxidation, enzyme inactivation and DNA cleavage. Identifying ROS and understanding their role is important to advance ACP applications to a range of complex microbiological issues. In this study, the inactivation efficacy of in-package, high voltage (80 kV_{RMS}) ACP (HVACP) and the role of intracellular ROS were investigated. Two mechanisms of inactivation were observed where reactive species were found to either react primarily with the cell envelope or to damage intracellular components. *E. coli* was inactivated mainly by cell leakage and low level DNA damage. Conversely, *S. aureus* was mainly inactivated by intracellular damage with significantly higher levels of intracellular ROS observed and little envelope damage. However, for both bacteria studied, increasing treatment time had a positive effect on intracellular ROS levels generated.

Keywords:

High voltage atmospheric cold plasma, in-package, intracellular ROS, cell leakage, DNA damage, *E. coli* and *S. aureus*

INTRODUCTION

Atmospheric cold plasma (ACP) refers to non-equilibrium plasma generated at near ambient temperatures and pressure. They are composed of particles including free electrons, radicals, positive and negative ions, but are low in collision frequency of gas discharging compared to equilibrium plasma (1, 2). ACP technologies have been widely applied for many surface treatments and environmental processes. Recently they have been studied for food sterilisation and plasma medicine (2-5).

ACP provides inactivation effects against a wide range of microbes, mainly by the generation of cell-lethal reactive species (6-8). By discharging in air, groups of reactive species are generated, such as reactive oxygen species (ROS), reactive nitrogen species (RNS), ultraviolet (UV) radiation, energetic ions and charged particles (5). However, the inactivation efficacy can be varied by changing the working gases which results in different types or amounts of reactive species generated (9-11). ROS are often identified as the principal affecting species with relatively long half-life and strong anti-microbial effects, which are generated in oxygen containing gases (12).

ROS generated during plasma discharge in air or oxygen-containing mixtures are assemblies of ozone, hydrogen peroxide, singlet and atomic oxygen, while ozone is considered as the most microbicidal specie (13). With strong oxidative stress, cells are damaged by lipid peroxidation, enzyme inactivation and DNA cleavage. Generating plasma in air or a nitrogen containing gas mixture can also generate NO_x species. However, a higher inactivation efficacy has been reported with the combined

application of NO and H₂O₂ on *E. coli* than a treatment with NO or H₂O₂ alone (14). Reactive nitrogen species are highly toxic and can lead to cell death by increasing DNA damage (15). One of the potential benefits of ACP as a sterilization or pasteurization technology is the reported low mutation level associated which may be attributed to the ‘cocktail’ of reactive species generated (16, 17). However, different patterns of cellular damage between Gram negative and positive bacteria were observed in former studies (18, 19). Moreover, the treatment parameter of mode of exposure has been previously described (13, 20), where the inactivation mechanism reported was similar in relation to direct or indirect exposure to the plasma. With regard to inactivation efficacy, indirect exposure to ACP had a reduced microbicidal effect where interaction with UV, electron beam, charged particles and other short-lived species was absent. However, the in-package treatment used in this study allows the contained recombination of reactive radicals, which could result in strong bactericidal effects, even with indirect exposure.

Thus, the inactivation mechanism of ACP is a possible result of the reactive species actions, which correlate to process and system parameters. Reactive species reactions with Gram negative and positive bacteria are potentially different. To prove this hypothesis, this study compared the inactivation mechanism of HVACP against *E. coli* and *S. aureus* to expand understanding of the possible different patterns of damage against Gram negative and Gram positive bacteria, especially the action of reactive oxygen species. The interactive effects of intracellular ROS generation and DNA damage with treatment time were examined in conjunction with spectral diagnostics

of the in package process to elucidate the mechanism.

MATERIALS AND METHODS

Bacterial Strains and Growth Conditions

The bacterial strains used in this study were *Escherichia coli* NCTC 12900 (non-toxigenic O157:H7) and *Staphylococcus aureus* ATCC 25923. Strains were chosen to represent both Gram negative and Gram positive bacteria and to facilitate comparison with other studies. They are pathogens of relevance to the food industry in addition to their multi-drug resistance and high rate of mutations (21, 22). *E. coli* NCTC 12900 was obtained from the National Collection of Type Cultures of the Health Protection Agency (HPA, UK), and *S. aureus* was obtained from the microbiology stock culture of the School of Food Science and Environmental Health, Dublin Institute of Technology. Strains were maintained as frozen stocks at -70 °C in the form of protective beads, which were plated onto tryptic soy agar (TSA, Scharlau Chemie, Barcelona, Spain) and incubated overnight at 37 °C to obtain single colonies before storage at 4 °C.

Preparation of Bacterial Cell Suspensions

Cells were grown overnight (18 h) by inoculating isolated colonies of respective bacteria in tryptic soy broth without glucose (TSB-G, Scharlau Chemie, Barcelona, Spain), at 37 °C. Cells were harvested by centrifugation at 8,720 g for 10 min. The cell pellet was washed twice with sterile phosphate buffered saline (PBS, Oxoid LTD, UK). The pellet was re-suspended in PBS and the bacterial density was determined by measuring absorbance at 550 nm using McFarland standard (BioMérieux,

100 Marcy-l'Étoile, France). Finally, cell suspensions with a concentration of 10^8 CFU
101 ml^{-1} were prepared in PBS.

102 **HVACP system configuration**

103 The dielectric-barrier discharge (DBD) HVACP system used in this study consists of a
104 high voltage transformer (with input voltage 230 V at 50 Hz), and a voltage variac
105 (output voltage controlled within 0~120 kV) (Figure 1). HVACP discharge was
106 generated between two 15-cm diameter aluminium electrodes separated by two
107 perspex dielectric layers (10 mm and 1mm thickness). The system was operated at
108 high voltage level of 80 kV_{RMS} at atmospheric pressure. Voltage and input current
109 characteristics of the system were monitored using an InfiniVision 2000 X-Series
110 Oscilloscope (Agilent Technologies Inc., USA). A polypropylene container, which
111 acted as both a sample holder and an additional dielectric barrier, was placed between
112 the two perspex dielectric layers. The distance between the two electrodes was kept
113 constant (2.2 cm) for all experiments.

114 **HVACP treatment**

115 For direct plasma treatment, 10 ml of bacterial cell suspensions in PBS were
116 aseptically transferred to a sterile plastic petri dish, which was placed in the centre of
117 the polypropylene container, between the electrodes. For indirect plasma treatment, a
118 separate container was used, where the sample petri dish was placed on the upper left
119 corner of the container, outside the plasma discharging area. Each container was
120 sealed in a high barrier polypropylene bag (B2630; Cryovac Sealed Air Ltd, Dunkan,
121 SC, USA) using atmospheric air as a working gas for HVACP generation. Bacterial

samples were then treated with HVACP at 80 kV_{RMS} for 1, 3 and 5 min. After HVACP treatment, samples were subsequently stored at room temperature for either 0, 1 or 24 h (23). Ozone concentrations were measured using GASTEC gas tube detectors (Product # 18M, Gastec Corporation, Kanagawa, Japan) immediately after treatment and also after 1 or 24 h storage. Containers were kept sealed to ensure the retention of contact with generated reactive species during post-treatment storage. Microbiological analysis were immediately applied after respective post-treatment storage. All experiments were carried out in duplicate and replicated twice.

Microbiological Analysis

To quantify the effects of plasma treatment, 1 ml of treated samples were serially diluted in maximum recovery diluent (MRD, Scharlau Chemie, Barcelona, Spain) and 0.1 ml aliquots of appropriate dilutions were surface plated on TSA. 1 ml and 0.1 ml of the treated sample was spread onto TSA plates as described by EN ISO 11290-2 method (ISO 11290-2, 1998). The limit of detection was 1 Log CFU ml⁻¹. Plates were incubated at 37 °C for 24 h and colony forming units were counted. Any plates with no growth were incubated for up to 72 h and checked for the presence of colonies every 24 h. Results are reported in Log CFU ml⁻¹ units.

Detection of reactive oxygen species after plasma treatment

DCFH (2',7'-dichlorodihydrofluorescein) is a cellular assay probe widely used for fluorescence detection of intracellular ROS. It revealed the concentration of ROS in HVACP treated samples.

After HVACP treatment and subsequent storage, cells were incubated with DCFH-DA

(2',7'-dichlorodihydrofluorescein diacetate, Sigma Aldrich Ltd, Dublin, Ireland) at a final concentration of 5 μ M in PBS for 15 min at 37 °C. Two hundred μ L aliquots of each sample were transferred into 96 well fluorescence microplate wells (Fisher Scientific, UK) and measured by SynergyTM HT Multi-Mode Microplate Reader (BioTek Instruments Inc.) at excitation and emission wave lengths of 485 and 525 nm.

Optical emission spectroscopy

Optical emission spectroscopy (OES) of the discharge within empty packages was acquired with an Edmund Optics UV Enhanced Smart CCD Spectrometer with an optical fibre input. UV Enhanced Smart CCD Spectrometers have been optimized for maximum performance in the ultraviolet and near UV region, and for multichannel operation with ultra-low trigger delay. The spectral resolution of the system was 0.6 nm.

The fibre optic from the spectrometer was placed facing towards the package to allow the light to cross the centre of the side wall of the polypropylene container. The fibre had a numerical aperture of 0.22 mm and was optimized for use in the ultraviolet, visible and near infrared portion of the spectrum with a wavelength range of 200 – 920 nm. A 5 mm diameter lens collected light from a column across the diameter of the package and focused it onto a 200 μ m multi-mode fibre. The other end of the 2 m long fibre was connected to the spectrometer.

Cell membrane integrity

Membrane integrity was examined by determination of the release of intracellular materials absorbing at 260 and 280 nm (A_{260} and A_{280}) (24). Untreated (bacterial cells

in PBS) and HVACP-treated samples were centrifuged at 13,200 g for 10 min. Untreated controls were used to determine the release of any intracellular material before HVACP treatment. Two hundred μ L supernatant of each sample was transferred into UV-transparent microtitre plate (Corning Life Science, US) wells and measured by SynergyTM HT Multi-Mode Microplate Reader at 260 nm and 280 nm.

DNA damage

To further examine intracellular damage, double-strand DNA (dsDNA) concentrations were investigated after 24 h storage, which provided adequate reaction time between ROS and cell components. SYBR Green I, [2-[N-(3-dimethylaminopropyl)-N-propylamino]-4-[2,3-dihydro-3-methyl-(benzo-1,3-thiazol-2-yl)-methylidene]-1-phenyl-quinolinium], is a highly sensitive detector of dsDNA and can be used to quantify nucleic acids. SYBR Green I has been widely used in fluorescence analysis, real-time PCR and biochip applications. (25) In this study, it was used as an indicator of DNA damage with a digested cell solution. Lysozyme and lysostaphin hydrolyse the bacterial cell wall by breaking 1-4 bonds between N-acetyl- β -D-glucosamine (NAG), N-acetyl- β -D-muramic acid (NAM) and polyglycine cross-links present in the peptidoglycan (26).

Following HVACP treatment *E. coli* samples were incubated with 100 μ g mL⁻¹ lysozyme at 37 °C for 4 h to break the cell envelope and release the intracellular DNA. Because of the different cellular structures in Gram positive bacteria, *S. aureus* samples were incubated with 100 μ g mL⁻¹ lysozyme and 10 μ g mL⁻¹ lysostaphin at 37 °C for 4 h. Cell digestion effects were verified by colony counts on TSA plates. Cells

without HVACP treatment were digested and used as positive control group, while untreated cells without digestion were used as negative controls. The bacterial envelope was considered as completely digested when the survival rate was below the detection level.

After cell digestion, solutions were incubated with SYBR Green I (1:10,000, Sigma Aldrich Ltd, Dublin, Ireland) at working concentration (1:1) for 15 min at 37 °C. 200 µL aliquots of each sample were transferred into 96 well fluorescence microplate wells (Fisher Scientific, UK) and measured by Synergy™ HT Multi-Mode Microplate Reader at excitation and emission wave lengths of 485 and 525 nm.

Scanning Electron Microscopy

Bacterial samples in PBS exposed to plasma for 1 min treatment with a post-treatment storage time of 1 or 24 h were selected for SEM analysis. This was based on a noticeable difference in plasma inactivation efficacy with respect to post-treatment storage time. Bacterial cells were prepared as described by Thanomsub *et al.* 2002 with minor modifications (27, 28). Samples were then examined visually by using a FEI Quanta 3D FEG Dual Beam SEM (FEI Ltd, Hillsboro, USA) at 5 kV.

Statistical Analysis

Statistical analysis was performed using SPSS 22.0 (SPSS Inc., Chicago, U.S.A.). Data represent the means of experiments performed in duplicate and replicated at least twice. Means were compared using analysis of variance (ANOVA) using Fisher's Least Significant Difference-LSD at the 0.05 level.

RESULTS

Effect of treatment time and post-storage time on plasma inactivation efficacy

The inactivation efficacy of HVACP against *E. coli* NCTC 12900 and *S. aureus* ATCC 25923 is shown in Tables 1 and 2. Inactivation was related to both treatment time and post-treatment storage time.

After 1 min exposure of HVACP, *E. coli* samples were decreased by around 2 log cycles in conjunction with 24 h post treatment storage. When treatment time was increased to 3 min, bacterial populations were undetectable for both 1 and 24 h storage times. Without post-treatment storage, approximately 3.6 and 2.3 log cycle reductions were detected with direct and indirect exposure after 3 min treatment, but further extending treatment time to 5 min resulted in 6 log cycle and at least 8 log cycle reductions for direct and indirect exposure respectively (Table 1, $p \leq 0.05$).

A similar trend of HVACP inactivation was recorded for *S. aureus*. With 24 h storage, all treatment times used led to undetectable levels of bacterial population, irrespective of the mode of exposure. Increasing treatment time, from 1 min to either 3 or 5 min, yielded undetectable levels, with direct and indirect exposure, respectively, after 1 h storage. With no post treatment storage time, populations declined by approximately 1.8 and 6.1 log cycles by increasing treatment time from 1 min to 5 min with direct exposure (Table 2, $p \leq 0.05$). Similar effects were achieved with indirect exposure.

Effect on cell membrane integrity

The absorbance of 260 and 280 nm which is commonly used for quantification of DNA and protein concentration, can also indicate the release of intracellular DNA and

protein and loss of cell integrity (24). Different trends between *E. coli* and *S. aureus* were observed from their absorbance measured at 260 nm following plasma treatment (Figure 2 and 3).

For *E. coli*, all absorption curves showed similar trends (Figure 2). With 24 h post-treatment storage, a sharp increase in absorbance followed by a steady stage indicated that the cell integrity was compromised within 1 min of HVACP treatment. In the case of 0 and 1 h post treatment storage samples, a sharp increase at 1 min of treatment was followed by a gradual increase in the absorbance as a function of treatment time ($p \leq 0.05$). In contrast, no leakage was recorded for *S. aureus*, even after 5 min treatment (Figure 3, $p > 0.05$). However, a small increase in absorbance was observed for the 24 h post treatment storage sample group for both control and treated samples. Similar trends were observed at 280 nm (data not shown).

Reactive oxygen and nitrogen species

The emission spectrum is presented in Figure 4 (a). Analysis of the discharge was carried out in air at 80 kV_{RMS} over the range of 200 - 920 nm. Distinct peaks obtained in the near UV and visible regions corresponded to strong emissions from N₂ and N₂⁺ excited species. The ozone concentration inside package after HVACP treatment was investigated using colorimetric tubes, which revealed its correlation with treatment and post-treatment storage time (Table 3). The in-package ozone densities were similar for each bacterial sample. Treatment time and post-treatment storage time had positive and negative effects respectively on the ozone concentration detected. Detected ozone concentration were not significantly different from containers of *E.*

254 *coli* or *S. aureus* samples with same treatment parameters. No ozone was detected in
255 either treatment condition after the 24 h post-treatment storage time. In air
256 DBD-ACPs, the well-known generation–depletion cycle of ozone is interlinked to that
257 of nitrogen oxides through several gas-phase reactions that generate N_2O , NO and O
258 atoms starting from O_2 and N_2^* (29). In Figure 4 (b), one of the major emission
259 intensity of second positive N_2 system from empty box and sample packages, where
260 other major peaks had similar results (data not shown).

261 The concentrations of ozone and nitrogen oxides (O_3 , NO_2 , NO_3 , N_2O_4) for this set-up
262 were quantified using absorption spectroscopy (OAS) and are reported elsewhere (29).
263 The measurements of ozone using the gas detectors compare with those reported
264 using OAS.

265 The oxidant-sensing fluorescent probe, DCFH-DA, is a nonpolar dye, which is
266 converted into the nonfluorescent polar derivative DCFH by cellular esterases and
267 switched to highly fluorescent DCF when oxidized by intracellular ROS and other
268 peroxides (30). It has been widely used for intracellular detection with fluorescence
269 analysis. The fluorescence signal correlated with the intracellular ROS density. Figure
270 5 shows the intracellular ROS density results of *E. coli* and *S. aureus* in PBS, where a
271 similar trend of ROS generation in response to HVACP is demonstrated for both
272 bacteria. With regard to the effect of mode of exposure, with indirect treatment the
273 ROS density increased gradually as a function of treatment time from 1 min to 5 min,
274 by comparison with direct treatment where ROS density was lower with prolonged
275 treatment.

DNA damage

Figure 6 presents the dsDNA quantity of *E. coli* and *S. aureus* before and after HVACP treatment. The control group from both bacteria obtained similar signal strength, which proved a similar initial DNA amount from samples. However, different signal levels were observed from the two treated strains. *E. coli* samples showed a reduction of fluorescence signal which correlated with treatment time. However, there was only a trace of fluorescence signal from *S. aureus* samples after treatment ($p \leq 0.05$).

Scanning Electron Microscopy

From the SEM results (Figure 7), more visible damage was evident on *E. coli* surfaces than *S. aureus*, indicating cell breakage effects for *E. coli* inactivation, while HVACP treatment caused irregular shape and cell shrinkage in *S. aureus*.

Proposed Inactivation Mechanism

Figure 8 illustrates the proposed mechanism of action of ACP with Gram negative and Gram positive bacteria based on the results described here for *E. coli* and *S. aureus*. After HVACP treatment, generated reactive oxygen species, associated with process and system parameters, attack both cell envelope and intracellular components. For Gram negative cells the cell envelope is the major target of ROS. Reactions of ROS with cell components cause disruption of the cell envelope and result in leakage, with some possible damage of intracellular components (eg. DNA). For Gram positive cells the intracellular components are the major target of ROS. Reactions of ROS will cause severe damage of intracellular components (eg. DNA), but not cell leakage.

Lower intracellular ROS in Gram negative bacteria can be result of both ROS depletion by cell envelope components and the cell leakage.

DISCUSSION

From the results of inactivation efficacy, there is clearly a strong effect of increasing treatment time, even without post treatment storage time. However, a surviving population could be below the detection limit with recovery possible during storage under some treatment and storage conditions. No further enrichment procedures were employed in this study. Incorporating a post-treatment storage time increased the inactivation efficacy significantly, especially with 24 h post-treatment storage time, which could be attributed to the amount of reactive species generated and their extended reaction time with bacteria (Tables 1 and 2). Similar results have been observed in our former studies (18). A post treatment storage time with retained antimicrobial efficacy has two-fold potential advantage, whereby the initial exposure could be minimal with enhanced efficacy during storage which is compatible with treatment of sensitive samples. Additionally a post treatment storage stage is compatible with many industrial processes. However, with applications to the food, beverage and pharmaceutical industries in mind, the strong oxidative effect with long HVACP exposure time could adversely affect some ingredients by inducing surface oxidation, which has been observed from ozone food sterilization technologies (31). A challenge for developing HVACP applications in the food industry is to optimize the dose or gas mixtures applied to ensure control of microbiological risks whilst

maintaining food quality characteristics.

A hypothetical mechanism of action of HVACP against *E. coli* and *S. aureus* were concluded as shown in Figure 8. Different reaction mechanism with ROS and cell components are discussed below from reactive species and cell damage results.

The leakage studies recorded pointed to different modes of action. High leakage levels were observed with all treatment and post-treatment storage steps for *E. coli* ($p \leq 0.05$), but not in *S. aureus* ($p > 0.05$) (Figure 2 and 3). The cell wall of Gram positive bacteria consists of peptidoglycan with tight structure and strength, while Gram negative bacteria are covered by a thin layer of peptidoglycan and an outer membrane of lipopolysaccharide. During plasma treatment, generated ROS can react with both lipopolysaccharide and peptidoglycan thus breaking the molecule structure by damaging C-O, C-N and C-C bonds. (32-34) However, an obvious leakage was only observed from *E. coli*. With the higher lipid content, lipid peroxidation may have taken place on lipopolysaccharides and resulted in the breakage of the cell envelope. (19) This could suggest that reactive species reacted with the cell wall in different patterns. Reactions with other cell wall components, such as peptidoglycan, could be also involved. Furthermore, Figure 7 visually illustrates the difference between *E. coli* and *S. aureus* after HVACP treatment and further supports our hypothesis on the pattern of damage. The effect of shrinkage but not breakage has also been reported on another Gram positive bacteria, *L. monocytogenes* (35).

As a main inactivation species, the ozone level inside the package showed strong correlation with treatment time and post-treatment storage time, but not with the type

of bacteria in the sample (Table 3). However, the fluorescent signal recorded for *S. aureus* was three times that of *E. coli*, thus indicating a much higher intracellular ROS density in *S. aureus* than for *E. coli* (Figure 5, $p \leq 0.05$). A similar time correlated ROS generation was reported by other researchers using a plasma jet treatment. Intracellular ROS increased over 5 min of treatment by air plasma from a jet (36), with a similar trend reported on generation of RNS (37). Plasma treatment time determines the input energy during discharging. As the key reactive species for oxygen containing working gases, the generation of ROS consumes most of the energy in air plasma. It has been suggested that in-package ROS can penetrate cell membranes by active transport across the lipid bilayer or transient opening of pores in the membrane (3). This could explain the correlation between treatment time and ozone/ intracellular ROS. The mode of exposure also adds complexity, where an obvious difference in reactive species was observed from OES and DCFH DA assay according to mode of exposure (Figure 4 and 5). Lower reactive species levels were detected from samples exposed to direct plasma than the indirectly exposed samples. This could be due to the quenching effect of liquid between electrodes on the ionizing of gases. However, similar inactivation levels and cell components damage were recorded. During direct treatment, undetectable ROS, mostly very short lived and transient species, might react immediately with cell components and be transformed. It appears cells were damaged by the relatively long lived species associated with indirect treatment, such as higher ozone levels.

After plasma discharging, the ozone concentrations in the gas phase were determined

to be independent of the type of bacteria, while intracellular ROS levels were strongly correlated with both process parameter and target bacteria characteristic. This could contribute to the different reaction and diffusion patterns of ROS to the cells. Based on the absorbance results at 260 nm in Figure 2 and 3, HVACP generated ROS could react with the cell wall rather than entering the cell in *E. coli* samples, whilst ROS accumulated inside the *S. aureus* cells.

E. coli samples showed a reduction of fluorescence signal of DNA correlating with treatment time in Figure 6. This trend elucidated that DNA damage has a plasma dose dependent pattern. There was only a trace of fluorescence signal from *S. aureus* samples post treatment, indicating greater DNA damage than with *E. coli*. It has been reported that plasma induced oxidative stress damage in *S. aureus* is due to intracellular oxidative reactions (38).

Overall, treatment time and post-treatment storage time had strong effects on inactivation efficacy against *E. coli* and *S. aureus* in this study, with a lower impact observed for mode of plasma exposure. The amount of reactive species generated, including ozone, has been correlated with inactivation efficacy (12, 36, 39-41).

Among the reactive species generated during HVACP treatment, ROS contributed as major antimicrobial factors. Their concentrations were governed by plasma dose and applied gas compositions (18). The generation of ozone as an indicator of ROS showed a time-dependent pattern, while intracellular ROS had a similar trend. During penetration, ROS could react with the lipid content in the cell membrane and cause certain damage. Compared with Gram positive bacteria, the membrane of Gram

negative bacteria was more vulnerable. Visible damage as a result of plasma exposure was previously observed for *E. coli* (13).

A much higher intracellular ROS density detected in *S. aureus* showed the probable penetration of reactive species within the cell. At the same time, higher concentrations of reactive species overall could lead to more intracellular damage to cell components such as DNA, which was clearly noted in this study. Since the total amount of ROS generated using any system or process setting is around the same level and is independent of the target bacteria characteristics, it is apparent that less cell envelope damage may be associated with more intracellular damage.

In this study, the HVACP inactivation efficacy of *E. coli* and *S. aureus* bacteria was correlated with process and system parameters (i.e. treatment time or post-treatment storage time). These determined the amount and reaction time of reactive species, which were the essential factors of antimicrobial reactions. Two different possible mechanisms of inactivation were observed in the selected Gram negative and Gram positive bacteria. Reactive species were either reacting with cell envelope or damaging intracellular components. *E. coli* was inactivated by cell envelope damage induced leakage, while *S. aureus* was mainly eliminated by intracellular damage. Additionally, the different cell damage mechanisms might due to different type of reactive species with regard to the mode of exposure. These findings are critical for the successful development of plasma applications where the system and process parameters can be nuanced in relation to the target risk characteristics presented.

Acknowledgements

408 The research leading to these results has received funding from the European
409 Community's Seventh Framework Program (FP7/2207-2013) under grant agreement
410 number 285820.

411 **Conflict of interest**

412 No conflict of interest.

Reference

1. **Bárdos L, Baránková H.** 2010. Cold atmospheric plasma: Sources, processes, and applications. *Thin Solid Films* **518**:6705-6713.
2. **Misra NN, Tiwari BK, Raghavarao KSMS, Cullen PJ.** 2011. Nonthermal plasma inactivation of food-borne pathogens. *IEEE Trans Plasma Sci* **30**:1409-1415.
3. **Sensenig R, Kalghatgi S, Cerchar E, Fridman G, Shereshevsky A, Torabi B, Arjunan KP, Podolsky E, Fridman A, Friedman G.** 2011. Non-thermal plasma induces apoptosis in melanoma cells via production of intracellular reactive oxygen species. *Ann Biomed Eng* **39**:674-687.
4. **Dobrynin D, Wasko K, Friedman G, Fridman AA, Fridman G.** 2011. Cold plasma sterilization of open wounds: live rat model. *Plasma Medicine* **1**:109-114.
5. **Cullen PJ, Milosavljević V.** 2015. Spectroscopic characterization of a radio-frequency argon plasma jet discharge in ambient air. *Prog Theor Exp Phys* **2015**:063J001.
6. **Kayes MM, Critzer FJ, Kelly-Wintenberg K, Roth JR, Montie TC, Golden DA.** 2007. Inactivation of foodborne pathogens using a one atmosphere uniform glow discharge plasma. *Foodborne Pathog Dis* **4**:50-59.
7. **Basaran P, Basaran-Akgul N, Oksuz L.** 2008. Elimination of *Aspergillus parasiticus* from nut surface with low pressure cold plasma (LPCP) treatment. *Food Microbiol* **25**:626-632.

- 435 8. **Klämpfl TG, Isbary G, Shimizu T, Li Y-F, Zimmermann JL, Stolz W,**
436 **Schlegel J, Morfill GE, Schmidt H-U.** 2012. Cold atmospheric air plasma
437 sterilization against spores and other microorganisms of clinical interest. Appl
438 Environ Microb **78**:5077-5082.
- 439 9. **Lerouge S, Wertheimer M, Marchand R, Tabrizian M, Yahia L.** 2000.
440 Effect of gas composition on spore mortality and etching during low-pressure
441 plasma sterilization. J Biomed Mater Res **51**:128-135.
- 442 10. **Purevdorj D, Igura N, Ariyada O, Hayakawa I.** 2003. Effect of feed gas
443 composition of gas discharge plasmas on *Bacillus pumilus* spore mortality.
444 Lett Appl Microbiol **37**:31-34.
- 445 11. **Zhang M, Oh JK, Cisneros-Zevallos L, Akbulut M.** 2013. Bactericidal
446 effects of nonthermal low-pressure oxygen plasma on *S. typhimurium* LT2
447 attached to fresh produce surfaces. J Food Eng **119**:425-432.
- 448 12. **Joshi SG, Cooper M, Yost A, Paff M, Ercan UK, Fridman G, Friedman G,**
449 **Fridman A, Brooks AD.** 2011. Nonthermal dielectric-barrier discharge
450 plasma-induced inactivation involves oxidative DNA damage and membrane
451 lipid peroxidation in *Escherichia coli*. Antimicrob Agents Chemother
452 **55**:1053-1062.
- 453 13. **Dobrynin D, Fridman G, Friedman G, Fridman A.** 2009. Physical and
454 biological mechanisms of direct plasma interaction with living tissue. New J
455 Phys **11**:115020.
- 456 14. **Boxhammer V, Morfill GE, Jokipii JR, Shimizu T, Klämpfl T, Li YF,**

- 457 **Köritzer J, Schlegel J, Zimmermann JL.** 2012. Bactericidal action of cold
458 atmospheric plasma in solution. *New J Phys* **14**:113042.
- 459 15. **Davies BW, Bogard RW, Dupes NM, Gerstenfeld TA, Simmons LA,**
460 **Mekalanos JJ.** 2011. DNA damage and reactive nitrogen species are barriers
461 to *Vibrio cholerae* colonization of the infant mouse intestine. *PLoS Pathog*
462 **7**:e1001295.
- 463 16. **Gaunt LF, Beggs CB, Georghiou GE.** 2006. Bactericidal action of the
464 reactive species produced by gas-discharge nonthermal plasma at atmospheric
465 pressure: a review. *IEEE Trans Plasma Sci* **34**:1257-1269.
- 466 17. **Boxhammer V, Li Y, Köritzer J, Shimizu T, Maisch T, Thomas H, Schlegel**
467 **J, Morfill G, Zimmermann J.** 2013. Investigation of the mutagenic potential
468 of cold atmospheric plasma at bactericidal dosages. *MUTAT RES-GEN TOX*
469 **EN 753**:23-28.
- 470 18. **Han L, Patil S, Keener KM, Cullen PJ, Bourke P.** 2014. Bacterial
471 inactivation by high-voltage atmospheric cold plasma: influence of process
472 parameters and effects on cell leakage and DNA damage. *J Appl Microbiol*
473 doi:10.1111/jam.12426:784-794.
- 474 19. **Laroussi M, Mendis DA, Rosenberg M.** 2003. Plasma interaction with
475 microbes. *New J Phys* **5**:41.41-41.10.
- 476 20. **Okubo M, Kuroki T, Miyairi Y, Yamamoto T.** 2004. Low-temperature soot
477 incineration of diesel particulate filter using remote nonthermal plasma
478 induced by a pulsed barrier discharge. *IEEE Trans Ind Appl* **40**:1504-1512.

- 479 21. **Braoudaki M, Hilton AC.** 2004. Low level of cross- resistance between
480 triclosan and antibiotics in *Escherichia coli* K-12 and *E. coli* O55 compared to
481 *E. coli* O157. FEMS Microbiol Lett **235**:305-309.
- 482 22. **Brown DF.** 2001. Detection of methicillin/oxacillin resistance in
483 staphylococci. J Antimicrob Chemother **48**:65-70.
- 484 23. **Ziuzina D, Patil S, Cullen PJ, Keener KM, Bourke P.** 2013. Atmospheric
485 cold plasma inactivation of *Escherichia coli* in liquid media inside a sealed
486 package. J Appl Microbiol **114**:778-787.
- 487 24. **Virto R, Manas P, Alvarez I, Condon S, Raso J.** 2005. Membrane damage
488 and microbial inactivation by chlorine in the absence and presence of a
489 chlorine-demanding substrate. Appl Environ Microbiol **71**:5022-5028.
- 490 25. **Zipper H, Brunner H, Bernhagen J, Vitzthum F.** 2004. Investigations on
491 DNA intercalation and surface binding by SYBR Green I, its structure
492 determination and methodological implications. Nucleic Acids Res
493 **32**:e103-e103.
- 494 26. **Goldman E, Green LH.** 2008. Practical handbook of microbiology. CRC
495 Press.
- 496 27. **Patil S, Valdramidis VP, Karatzas KAG, Cullen PJ, Bourke P.** 2011.
497 Assessing the microbial oxidative stress mechanism of ozone treatment
498 through the responses of *Escherichia coli* mutants. J Appl Microbiol
499 **111**:136-144.
- 500 28. **Thanomsub B, Anupunpisit V, Chanphetch S, Watcharachaipong T,**

501 **Poonkhum R, Srisukonth C.** 2002. Effects of ozone treatment on cell growth
502 and ultrastructural changes in bacteria. *J Gen Appl Microbiol* **48**:193-199.

503 29. **Moiseev T, Misra N, Patil S, Cullen P, Bourke P, Keener K, Mosnier J.**
504 2014. Post-discharge gas composition of a large-gap DBD in humid air by
505 UV–Vis absorption spectroscopy. *Plasma Sources Sci T* **23**:065033.

506 30. **Gomes A, Fernandes E, Lima JLFC.** 2005. Fluorescence probes used for
507 detection of reactive oxygen species. *J Biochem Biophys Methods* **65**:45-80.

508 31. **Kim J-G, Yousef AE, Dave S.** 1999. Application of ozone for enhancing the
509 microbiological safety and quality of foods: a review. *J Food Prot*
510 **62**:1071-1087.

511 32. **Chung TY, Ning N, Chu JW, Graves DB, Bartis E, Seog J, Oehrlein GS.**
512 2013. Plasma deactivation of endotoxic biomolecules: vacuum ultraviolet
513 photon and radical beam effects on lipid A. *Plasma Process Polym*
514 **10**:167-180.

515 33. **Yusupov M, Neyts E, Khalilov U, Snoeckx R, Van Duin A, Bogaerts A.**
516 2012. Atomic-scale simulations of reactive oxygen plasma species interacting
517 with bacterial cell walls. *New J Phys* **14**:093043.

518 34. **Yusupov M, Bogaerts A, Huygh S, Snoeckx R, van Duin AC, Neyts EC.**
519 2013. Plasma-induced destruction of bacterial cell wall components: a reactive
520 molecular dynamics simulation. *J Phys Chem C* **117**:5993-5998.

521 35. **Cullen PJ, Misra N, Han L, Bourke P, Keener K, O'Donnell C, Moiseev T,**
522 **Mosnier JP, Milosavljevic V.** 2014. Inducing a Dielectric Barrier Discharge

523 Plasma Within a Package. IEEE Trans Plasma Sci **42**:2368-2369.

524 36. **Ali A, Kim YH, Lee JY, Lee S, Uhm HS, Cho G, Park BJ, Choi EH.** 2014.

525 Inactivation of *Propionibacterium acnes* and its biofilm by non-thermal

526 plasma. Curr Appl Phys.

527 37. **Cheng X, Sherman J, Murphy W, Ratovitski E, Canady J, Keidar M.**

528 2014. The effect of tuning cold plasma composition on glioblastoma cell

529 viability. PLoS one **9**:e98652.

530 38. **Zhang Q, Liang Y, Feng H, Ma R, Tian Y, Zhang J, Fang J.** 2013. A study

531 of oxidative stress induced by non-thermal plasma-activated water for

532 bacterial damage. Appl Phys Lett **102**:203701.

533 39. **Arjunan KP, Friedman G, Fridman A, Clyne AM.** 2012. Non-thermal

534 dielectric barrier discharge plasma induces angiogenesis through reactive

535 oxygen species. J R Soc Interface **9**:147-157.

536 40. **Ishaq M, Kumar S, Varinli H, Han Z, Rider AE, Evans MD, Murphy AB,**

537 **Ostrikov KK.** 2014. Atmospheric gas plasma-induced ROS production

538 activates TNF-ASK1 pathway for the induction of melanoma cancer cell

539 apoptosis. Mol Biol Cell:mbc. E13-10-0590.

540 41. **Brun P, Vono M, Venier P, Tarricone E, Deligianni V, Martines E, Zuin M,**

541 **Spagnolo S, Cavazzana R, Cardin R, Castagliuolo I, Valerio AL, Leonardi**

542 **A.** 2012. Disinfection of ocular cells and tissues by atmospheric-pressure cold

543 plasma. PLoS One **7**:e33245.

544

Tables and Figures

Table 1. Surviving cell numbers of *E. coli* NCTC 12900 with respect to treatment and post-treatment storage time

Post-treatment storage time (h)	Plasma treatment time (min)	Mode of Plasma Exposure			
		Direct		Indirect	
		Cell density (Log ₁₀ CFU/ml)	SD*	Cell density (Log ₁₀ CFU/ml)	SD*
0	0	8.0 ^a	0.0	8.0 ^a	0.0
	1	7.6 ^a	0.1	7.3 ^b	0.1
	3	4.3 ^b	0.1	5.7 ^c	0.1
	5	2.1 ^c	0.7	ND* ^d	0.0
1	0	8.0 ^a	0.0	8.0 ^a	0.0
	1	7.2 ^d	0.1	7.1 ^b	0.2
	3	ND ^e	0.0	ND ^d	0.0
	5	ND ^e	0.0	ND ^d	0.0
24	0	8.0 ^a	0.0	8.0 ^a	0.0
	1	5.9 ^{df}	0.1	6.1 ^{be}	0.8
	3	ND ^e	0.0	ND ^d	0.0
	5	ND ^e	0.0	ND ^d	0.0

Different letters indicate a significant difference at the 0.05 level between different treatment times and post-treatment storage times

Critical controls were provided as 0 min treated samples with 0, 1 and 24 h post-treatment storage.

SD*: Standard deviation

ND*: Under detection limit

Table 2. Surviving cell numbers of *S. aureus* ATCC 25923 with respect to treatment and post-treatment storage time

Post-treatment storage time (h)	Plasma treatment time (min)	Mode of Plasma Exposure			
		Direct		Indirect	
		Cell density (Log ₁₀ CFU/ml)	SD*	Cell density (Log ₁₀ CFU/ml)	SD*
0	0	7.9 ^a	0.2	7.9 ^a	0.2
	1	6.1 ^b	0.3	5.8 ^b	0.3
	3	5.4 ^c	0.6	5.3 ^c	0.1
	5	1.8 ^d	0.2	1.7 ^d	0.1
1	0	7.8 ^a	0.2	7.8 ^a	0.2
	1	4.3 ^{bf}	0.0	2.0 ^{bf}	0.0
	3	ND ^e	0.0	ND ^e	0.0
	5	ND ^e	0.0	ND ^e	0.0
24	0	7.8 ^a	0.2	7.8 ^a	0.2
	1	ND ^e	0.0	ND ^e	0.0
	3	ND ^e	0.0	ND ^e	0.0
	5	ND ^e	0.0	ND ^e	0.0

Different letters indicate a significant difference at the 0.05 level between different treatment times and post-treatment storage times

Critical controls were provided as 0 min treated samples with 0, 1 and 24 h post-treatment storage.

SD*: Standard deviation

ND*: Under detection limit

563 Table 3. In-package ozone concentration after different HVACP treatment and
 564 post-treatment storage time with both *E. coli* and *S. aureus* samples

Post-treatment storage time (h)	Plasma treatment time (min)	Ozone concentration (ppm)	
		Direct	Indirect
0	1	1600	1800
	3	2400	3000
	5	4200	4400
1	1	100	120
	3	180	190
	5	330	350
24	1	ND	ND
	3	ND	ND
	5	ND	ND

565 ND*: Non-detectable

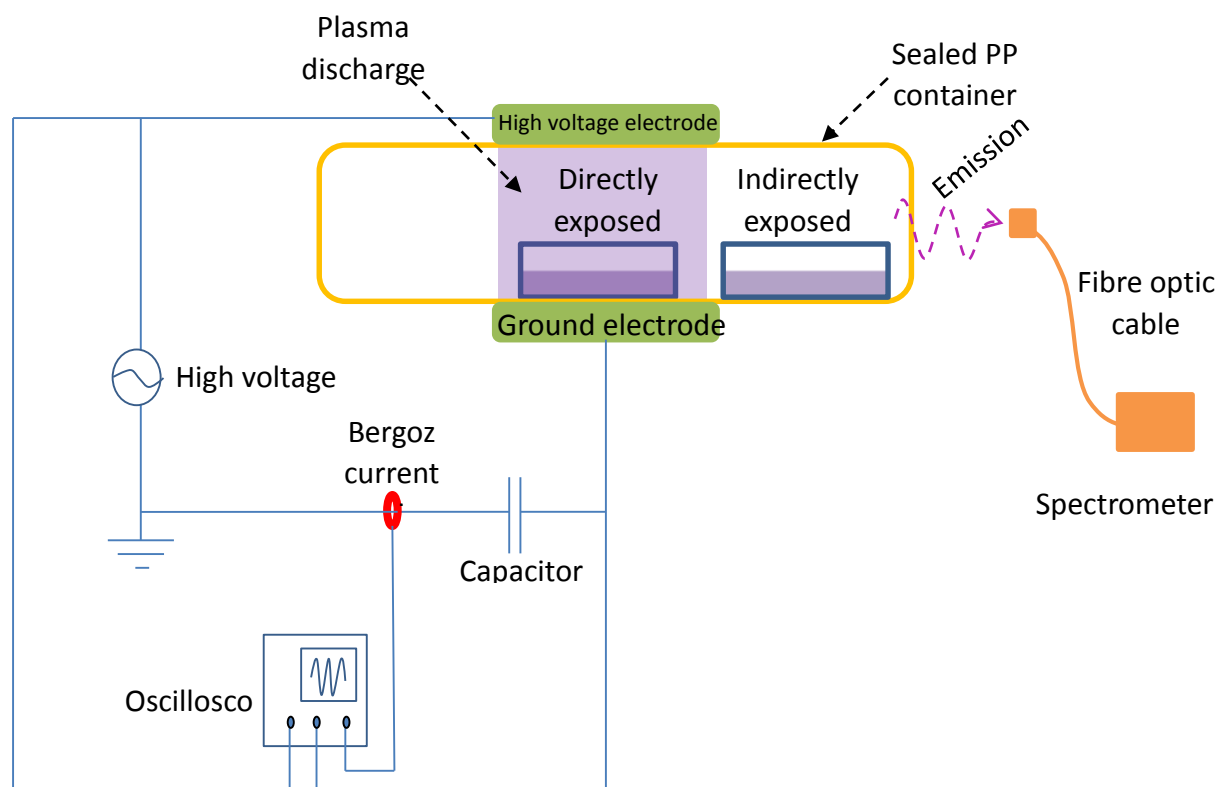


Figure 1. A schematic diagram of the DIT120+ HVACP device.

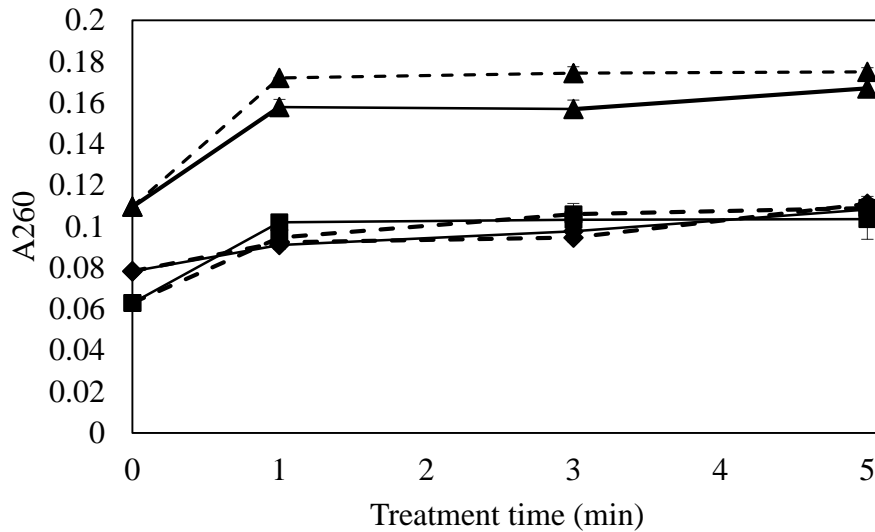


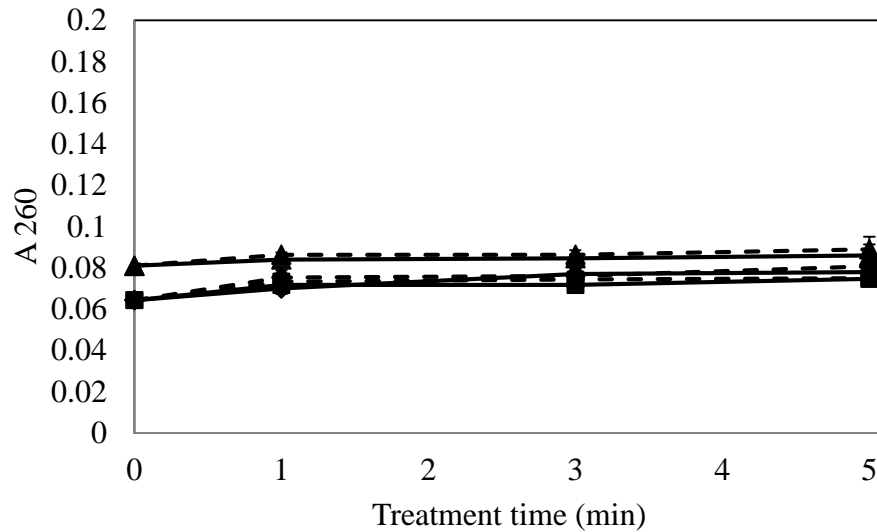
Figure 2. Absorbance of HVACP treated *E. coli* NCTC 12900 suspension in PBS at 260 nm with different post-treatment storage times

Data points at 0 min treatment time refer to untreated control stored with 0, 1, 24 h in PBS

1, 3, 5 min treatment at 80 kV_{RMS} with 0, 1, 24 h post-treatment storage

(■ 0 h post-treatment storage time; ♦ 1 h post-treatment storage time; ▲ 24 h post-treatment storage time)

(Solid line: direct exposure; Dotted line: indirect exposure)



577

578 Figure 3. *S. aureus* ATCC 25923 absorbance at 260 nm after HVACP treatment in

579 PBS

580 Data points at 0 min treatment time refer to untreated control stored with 0, 1, 24 h in

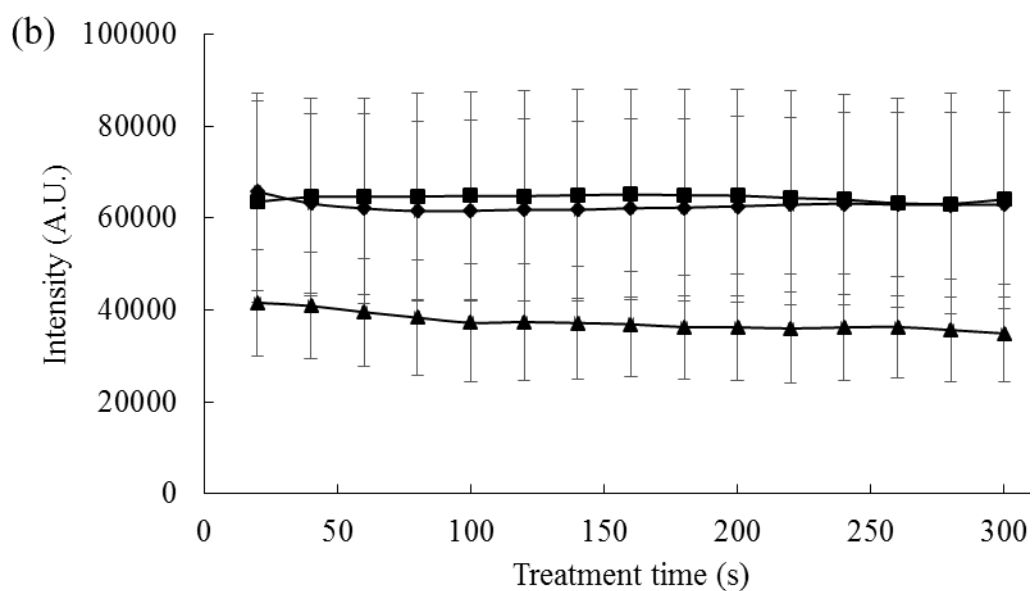
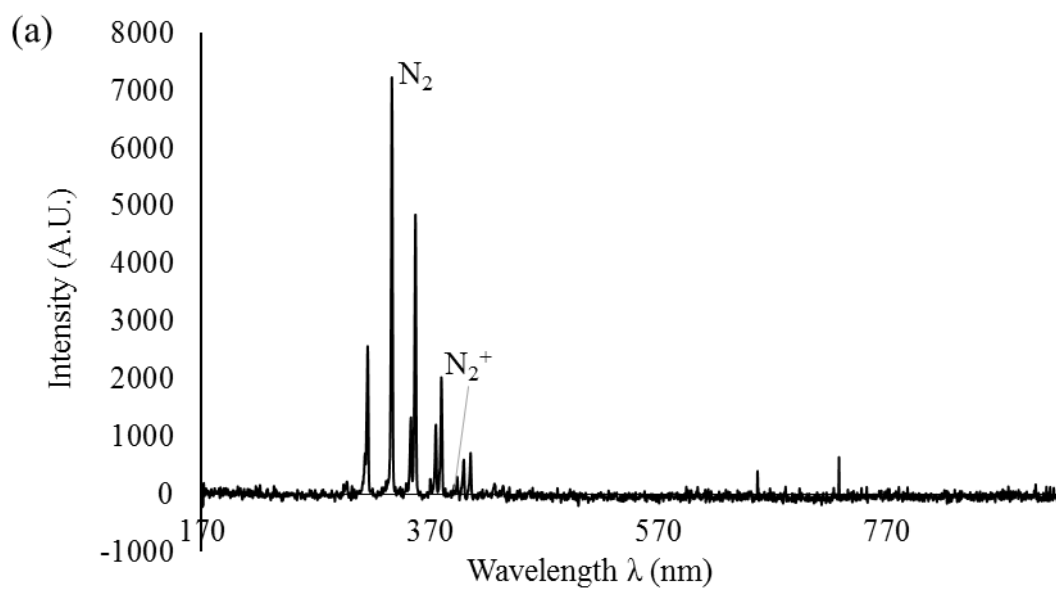
581 PBS

582 1, 3, 5 min treatment at 80 kV_{RMS} with 0, 1, 24 h post-treatment storage

583 (■ 0 h post-treatment storage time; ♦ 1 h post-treatment storage time; ▲ 24 h

584 post-treatment storage time)

585 (Solid line: direct exposure; Dotted line: indirect exposure)



586

587 Figure 4. Emission spectrum of dielectric barrier discharge atmospheric cold plasma

588 operating in air under atmospheric pressure

589 (a) Emission spectrum of empty box

590 (b) Emission intensity at 336.65 nm (■ Empty box; ▲ Direct exposure; ♦ Indirect

591 exposure.)

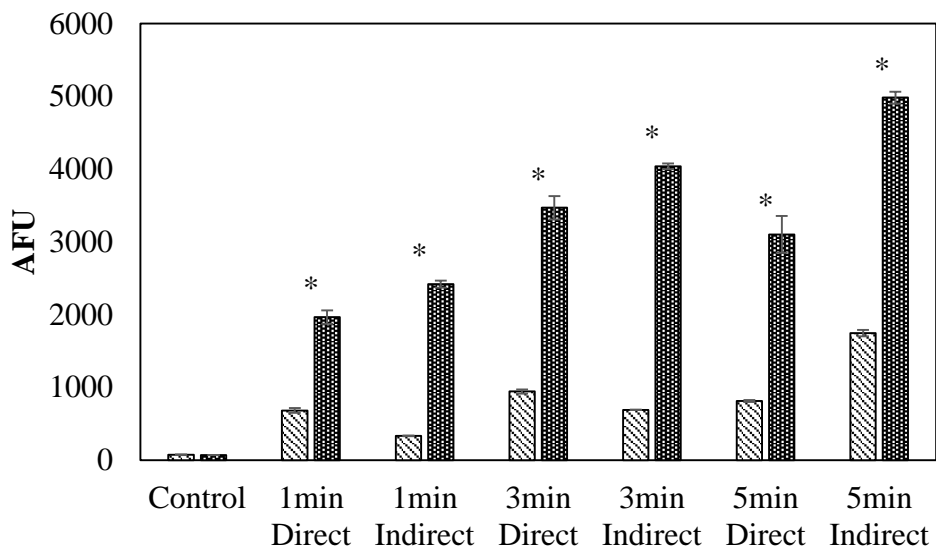


Figure 5. *E. coli* NCTC 12900 and *S. aureus* ATCC 25923 Intracellular ROS density assay by DCFH DA

1, 3, 5 min treatment at 80 kV_{RMS} with 0 h post-treatment storage

(▨ *E. coli* NCTC 12900; ▤ *S. aureus* ATCC 25923)

* indicate a significant difference at the 0.05 level between *E. coli* and *S. aureus*

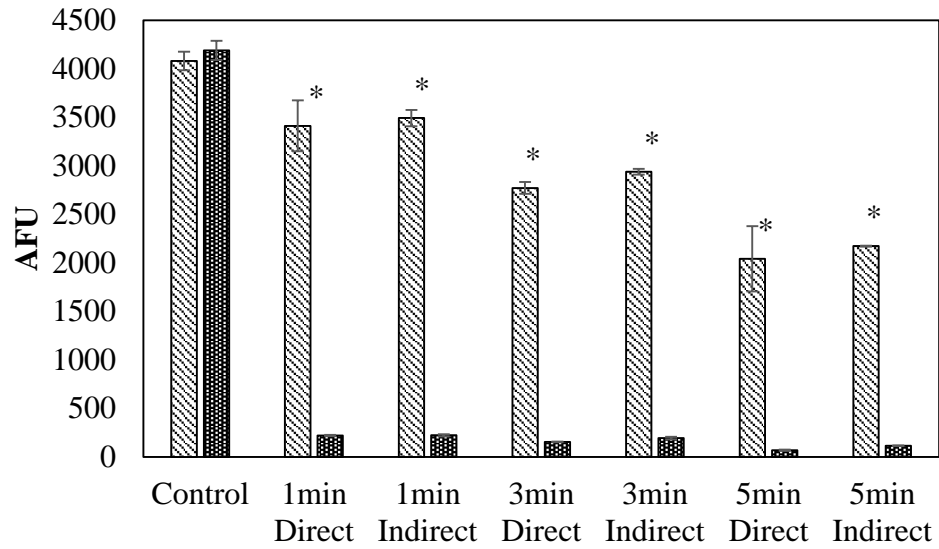


Figure 6. *E. coli* NCTC 12900 and *S. aureus* ATCC 25923 DNA quantification assay by SYBR Green 1

1, 3, 5 min treatment at 80 kV_{RMS} with 24 h post-treatment storage

(▨ *E. coli* NCTC 12900; ■ *S. aureus* ATCC 25923)

* indicate a significant difference at the 0.05 level between *E. coli* and *S. aureus*

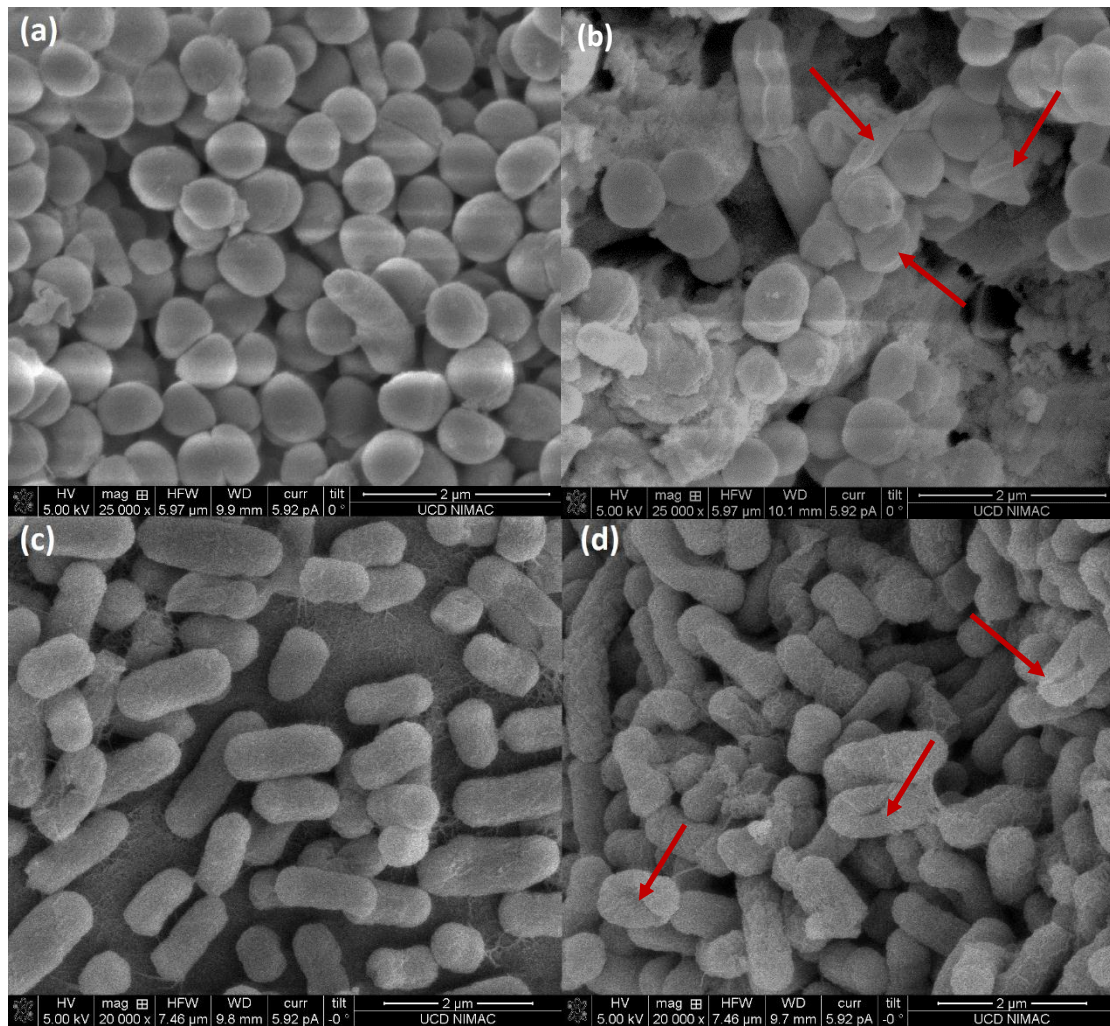


Figure 7. SEM images of control and treated cells with 80 kV_{RMS} 1 min indirect plasma exposed following 24 h post-treatment storage

(a) Untreated *S. aureus* ATCC 25923

(b) Treated *S. aureus* ATCC 25923

(c) Untreated *E. coli* NCTC 12900

(d) Treated *E. coli* NCTC 12900

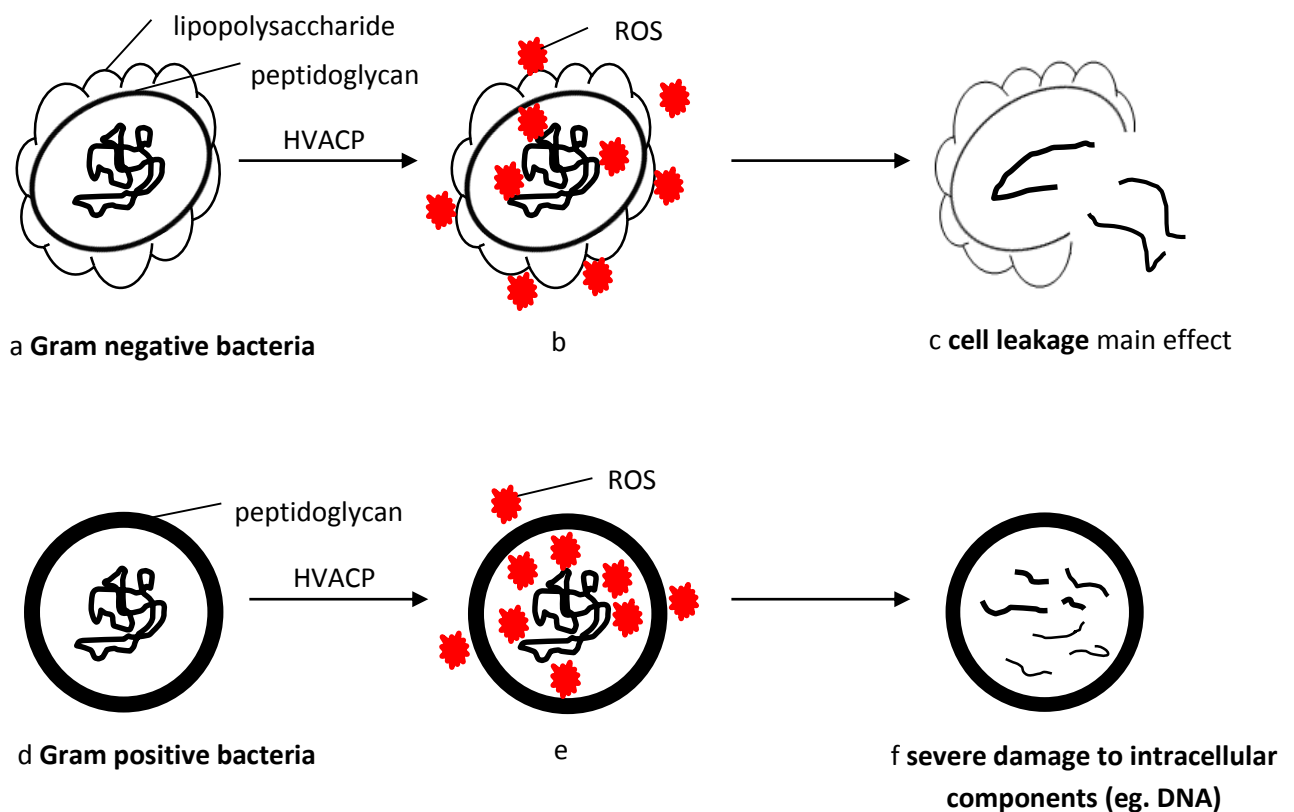


Figure 8. Proposed mechanism of action of HVACP with Gram negative and positive bacteria

a, b, c the proposed inactivation mechanism of Gram negative bacteria: a, structure of Gram negative bacteria before treatment, cell envelope consists of thin layer of peptidoglycan and lipopolysaccharide; b, ACP generated ROS attacking both cell envelope and intracellular components, where cell envelope is the major target; c, inactivation mainly caused by cell leakage, with some DNA damage possible.

c, d, e the proposed inactivation mechanism of Gram positive bacteria: c, structure of Gram positive bacteria before treatment, cell envelope consist a thick rigid layer of peptidoglycan; d, ACP generated ROS attacking both cell envelope and intracellular components, where intracellular materials are the major targets; e, inactivation mainly caused by intracellular damage (eg. DNA breakage), but not leakage.